Journal of Agrometeorology

(A publication of Association of Agrometeorologists)

ISSN : 0972-1665 (print), 2583-2980 (online)

Vol. No. 28 (3) : 366-374 (September - 2026)

https://doi.org/10.54386/jam.v28i3.3575

https://journal.agrimetassociation.org/index.php/jam

Research paper

Spatio-Temporal Assessment of Land Use/Land Cover Change, Land Surface Temperature, and Groundwater Fluctuations Using Remote Sensing and GIS: A Case Study of Ghaziabad District

SADAF

PG Department of Geography, Veer Kunwar Singh University, Ara, Bihar, India

Correspondence author email: sadafmalik849@gmail.com

ABSTRACT

Urbanization has been increasing at a rapid rate, which has led to transformation in the land use/land cover (LULC) and thus has a significant impact on groundwater resources and land surface temperature (LST) in rapidly developing cities. The present study aims to identify the spatio-temporal dynamics of LULC, LST, and the variability of groundwater in Ghaziabad District, Uttar Pradesh, India, from 2013 to 2023 using Remote Sensing and GIS techniques. Multi-temporal Landsat data were classified using the Maximum Likelihood Supervised Classification algorithm for the LULC maps that included 5 classes: built-up area, agriculture, vegetation, barren land, and water bodies. The accuracy of the classifications was assessed by the Kappa coefficient, and the Ordinary Kriging (OK) method was applied to spatially interpolate the groundwater depth in ArcGIS 10.8. Between 2013 and 2023, substantial increases in built-up areas and loss of vegetation cover were observed in the findings. Over the same time period, groundwater depth continued to decline in a progressive manner, and high LST areas became larger, especially in dense urban settings. The integrated analysis shows that surface thermal conditions and groundwater stress have intensified due to LULC transformation. The results highlight the importance of sustainable urban planning, groundwater recharge initiatives, and green infrastructure to reduce thermal risks and promote environmental sustainability in rapidly urbanizing areas.

***Keywords*:** Land use land cover, Accuracy assessment, Groundwater fluctuation, Urbanization, Geographic information system

Land use/land cover (LULC) change is one of the most important factors that influence ecosystem functions, water resources, and urban thermal environment (Battista & De Lieto Vollaro, 2017). The transformation of vegetated landscapes, forests, and agricultural fields to impervious built-up areas changes the surface energy balance, leading to an increase in land surface temperature (LST), urban heat islands, and environmental degradation (Saha *et al.,* 2024). The anthropogenic heat emissions, vegetation loss, and rapid urbanization and industrialization further amplify thermal stress by decreasing the evapotranspiration cooling effect (Moharir *et al.,* 2025). Groundwater resources are also at risk as a result of urbanization and climate change, as these influences alter infiltration, runoff, interception, and overall hydrological balance, which can lead to less groundwater recharge and impacts to groundwater quality (Wang *et al.,* 2018). Another example is that permeable surfaces are replaced with impervious surfaces, further exacerbating groundwater loss and increasing runoff and water demand (Patra *et al.,* 2018; Zahran *et al.,* 2023). Ghaziabad District of the National Capital Region (NCR) in India has been witnessing rapid urbanization, industry growth, and population growth in the past decade. Groundwater is a major source of domestic, agricultural, and industrial water requirements, but over-exploitation of groundwater and reduced recharge have put tremendous strain on the aquifer systems (Tyagi & Sharma, 2021). The Central Ground Water Board (CGWB, 2023) reported that extraction of groundwater increased by 123% and the depth of groundwater also rose from 24.9 m in 2016 to 33 m in 2023, signifying a high level of groundwater depletion. The reduction in vegetation and agricultural land cover from built-up areas has also been observed in previous studies, which have shown an increase in LST and environmental stress (Singh & Mishra, 2020; Anand *et al.,* 2024). Previous studies have focused on the relationship between LULC and LST or between

***Article info - DOI*:** *https://doi.org/10.54386/jam.v28i3.3575*

Received:22 June 2026; Accepted: 11 August 2026; Published online : 7 September 2026

LST and groundwater dynamics, and fewer studies have considered them together, with a focus on spatio-temporal interactions. The novelty of this study is the integrated assessment of the seasonal LULC change, LST variation, and groundwater fluctuation using multi-temporal Landsat images and groundwater observation data for 2013 and 2023. The goals of the study are: (i) to evaluate the LULC change, (ii) to quantify the seasonal and temporal change in LST, (iii) to evaluate the groundwater fluctuations, and (iv) to study spatio-temporal pattern analysis and spatial correspondence between land use/land cover change, land surface temperature, and groundwater changes. It is believed that the temperature and impervious surface of the landscape have increased over time and have played a role in groundwater depletion over the study period.

Study Area: Ghaziabad District

Ghaziabad District lies in the western part of Uttar Pradesh, India, in the National Capital Region (NCR) between 28°36′–28°55′ N and 77°12′–77°42′ E (Fig. 1). Ghaziabad was chosen for the study because of its rapid urbanization, LULC change, rising land surface temperature, groundwater stress and its location in the Ganga–Yamuna Doab, which is one of the fastest growing urban and industrial districts of India, while peri-urban areas in Ghaziabad are dominated by agriculture. The climate in the district is tropical, characterized by hot summers, cool winters, and monsoon season. The principal surface water bodies are the Hindon River (a tributary of the Yamuna River). Groundwater is the main source of water for domestic, agricultural, and industrial purposes. Groundwater depth continued to deplete, with an average groundwater depth of 29.93 mbgl (2022) compared to 28.96 mbgl (2020) (UPGWD, 2022).

MATERIAL AND METHODS

Data Used

In order to fulfil the objectives of the research, LULC and LST distribution maps were generated using multi-temporal, cloud-free Landsat-8 OLI datasets for the years 2013–2023 that were collected from the United States Geological Survey (USGS) (http://earthexplorer.usgs.gov) (Fig. 2). All datasets have a 30 m spatial resolution. The WGS-84 datum was used to project all datasets to the Universal Transverse Mercator 44-N projection. Each of the images was retrieved for the same season with the lowest time interval in order to avoid seasonal variations in the study area. ERDAS Imagine 15 software was utilized for change detection, classification, and image processing. For the LST distribution of the research area, ArcGIS 10.8 software was used. Groundwater depth data were acquired from the Central Ground Water Board (CGWB) and India-WRIS. The groundwater depth data were taken from four long-term CGWB monitoring piezometers (Modi Nagar-Pz I, Modi Nagar-Pz II, Morta Pz GWD, Bhojpur-Pz) with continuous observations for both 2013 and 2023. Spatial coverage of the monitoring network was limited; however, these stations were chosen as representative of the long-term observations available for the study period. Table 1 provides details of the satellite data that were collected.

Preparation of LULC classification maps

LULC classifications were performed using multispectral Landsat images from 2013 to 2023. After LANDSAT data pre-processing, land use classification was carried out. Five classifications of LULC maps of Ghaziabad district were identified: built-up, vegetation, barren, agriculture, and water bodies. A supervised maximum likelihood method was applied to the categorization of raster images using ERDAS Imagine 15. The land use change matrix from 2013 to 2023 was used in this research to detect LULC changes for Ghaziabad district. Using the change matrix throughout the study period, the rates of LULC alteration, loss, and gain of the study region were calculated.

Accuracy Assessment

Evaluating the accuracy of LULC categorization is an essential step in determining its reliability and quality. The extent of agreement between the reference data and the map's classification is shown by a statistic called the Kappa Coefficient. The Kappa coefficient technique, which computes the accuracy of user, producer, and overall classification and provides the Kappa coefficient index (k), is used in the study to evaluate the accuracy of land use land cover maps for the Ghaziabad district. In order to ensure an equal representation of all LULC classes over the whole study area, 330 randomly selected locations were thoroughly selected. Signatures, or training data, were created utilizing Google Earth Pro. Using the formula below, the accuracy of overall categorization of the land use and land cover maps for 2013 and 2023 has been assessed (Cohen, 1960).

$$\mathrm{K} = \mathrm{Pra} - \mathrm{Pr(e)}/1 - \mathrm{Pr(e)} \quad \text{……………….(1)}$$

Where, Pr(a) = The actual observed agreement, Pr(e) = The Chance agreement

LST retrieval for the years 2013 and 2023

In the present research, the NDVI of the Ghaziabad district was calculated utilizing the OLI spectral bands 2, 3, 4, and 5, while the brightness temperature was estimated using the TIR band 10 (Fig. 2). The thermal constant, rescaling factor value, and other band metadata are provided by Landsat 8 and can be utilized for calculations such as LST. The following are the processes for land surface temperature estimation.

1- Calculation of TOA (Top of Atmospheric) spectral radiance

The metadata file's radiance rescaling parameters were used to change the thermal band data DN to TOA spectral radiance.

$$\mathrm{TOA(L)} = \mathrm{M_L} * \mathrm{Q_{cal}} + \mathrm{A_L} - \mathrm{O_i} \quad \text{……………….(2)}$$

Where, L represents the top of atmospheric spectral indices, ML is band-specific multiplicative rescaling factor Qcal is Band 10 imagery, AL is band-specific additive rescaling factor, Oi is the correction for Band 10'

2- TOA to the Brightness Temperature conversion

The thermal constant values in the metadata file can be used to convert spectral radiance data to the top of atmospheric brightness temperature (Ramaiah *et al.,* 2020).

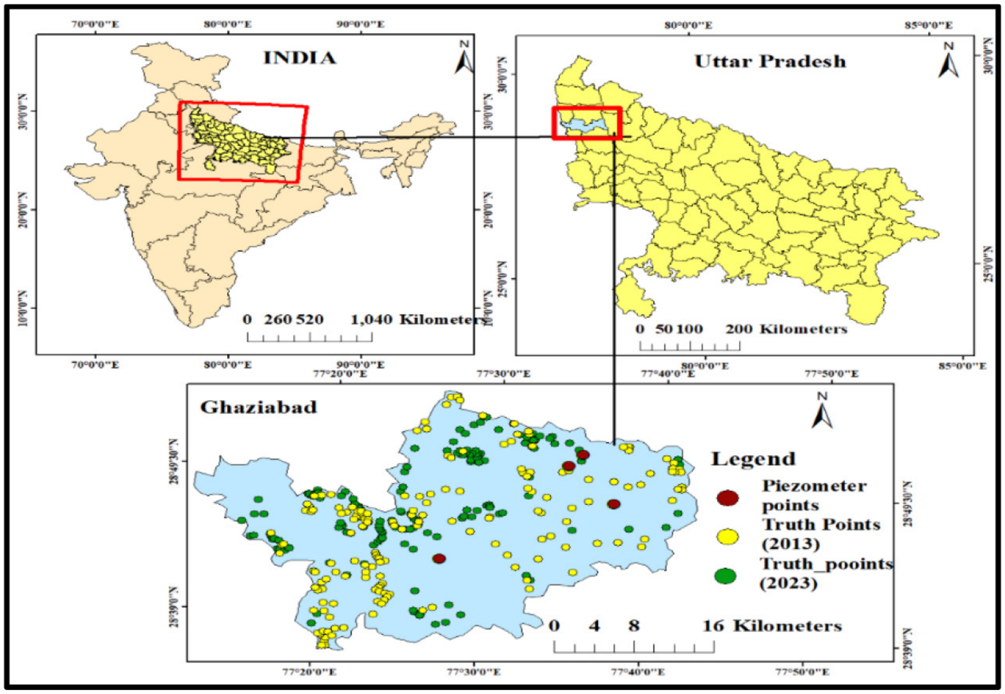

Fig. 1: Study area

Table 1: Data used for LULC, land surface temperature and groundwater depth

S. No.	Data Used	Acquisition Date(s)	Bands Used	Purpose	Source
1	Landsat 8 OLI/ TIRS	13 May 2013 (Summer), 21 November 2013 (Winter), 09 May 2023 (Summer), 17 November 2023 (Winter)	Band 2 (Blue, 0.45–0.51 µm), Band 3 (Green, 0.53–0.59 µm), Band 4 (Red, 0.64–0.67 µm), Band 5 (Near Infrared, 0.85–0.88 µm), Band 6 (SWIR-1, 1.57–1.65 µm), Band 7 (SWIR-2, 2.11–2.29 µm), Band 10 (Thermal Infrared, 10.60–11.19 µm)	Preparation of Land Use/Land Cover (LULC) maps and Land Surface Temperature (LST) estimation	USGS Earth Explorer
2	Groundwater depth	May 2013, November 2013, May 2023, November 2023	Observation well (Piezometer) data	Groundwater depth analysis and spatial interpolation	India-WRIS & Central Ground Water Board (CGWB)

$$\mathrm{BT} = \left(\frac{K_2}{\ln\left(\frac{K_1}{L}\right)+1}\right) - 273.15 \qquad \ldots\ldots\ldots\ldots\ldots\ldots(3)$$

Where, $K1$ and $K2$ = Band-specific thermal conversion constants, L = TOA spectral radiance (Watts/(m2 * sr * µm)), Thermal constant, Band 10: $K1$= 1321.08 and $K2$= 777.89

3- Calculate the NDVI

NDVI values were computed using Landsat 8-OLI's RED and NIR band. It is employed to evaluate the vegetation cover's health. The emissivity and proportion of vegetation can be computed with the use of the NDVI calculation (Rouse *et al.,* 1974). Each of these metrics is crucial to the LST computation.

$$\mathrm{NDVI} = (\mathrm{NIR} - \mathrm{RED})/(\mathrm{NIR} + \mathrm{RED}) \ldots\ldots\ldots\ldots\ldots\ldots(4)$$

Where, RED represents the digital number values from the Band 4, NIR represents the digital number values from the Band 5.

4- Calculate the proportion of vegetation P_v

The proportion of ground area covered by vegetation is known as the vegetation proportion in a vertical projection. Through surface albedo, emissivity, roughness, and changes in vegetation cover and plant transpiration have a direct effect on energy budgets and surface water (Aman *et al.,* 1992). The traditional NDVI approach was used in this study for estimating PV (Carlson & Ripley, 1997).

$$P_v = \mathrm{Square}((\mathrm{NDVI} - \mathrm{NDVI_{min}})/(\mathrm{NDVI_{max}} - \mathrm{NDVI_{min}})) \ldots\ldots\ldots\ldots\ldots\ldots(5)$$

Where, NDVI= Normalized difference vegetation index, $\mathrm{NDVI_{min}}$= Minimum value of the NDVI, $\mathrm{NDVI_{max}}$= Maximum value of the NDVI

5- Calculate Emissivity (ε)

The NDVI, which is derived from the brightness that a certain location emits, is a feature of natural objects and a significant

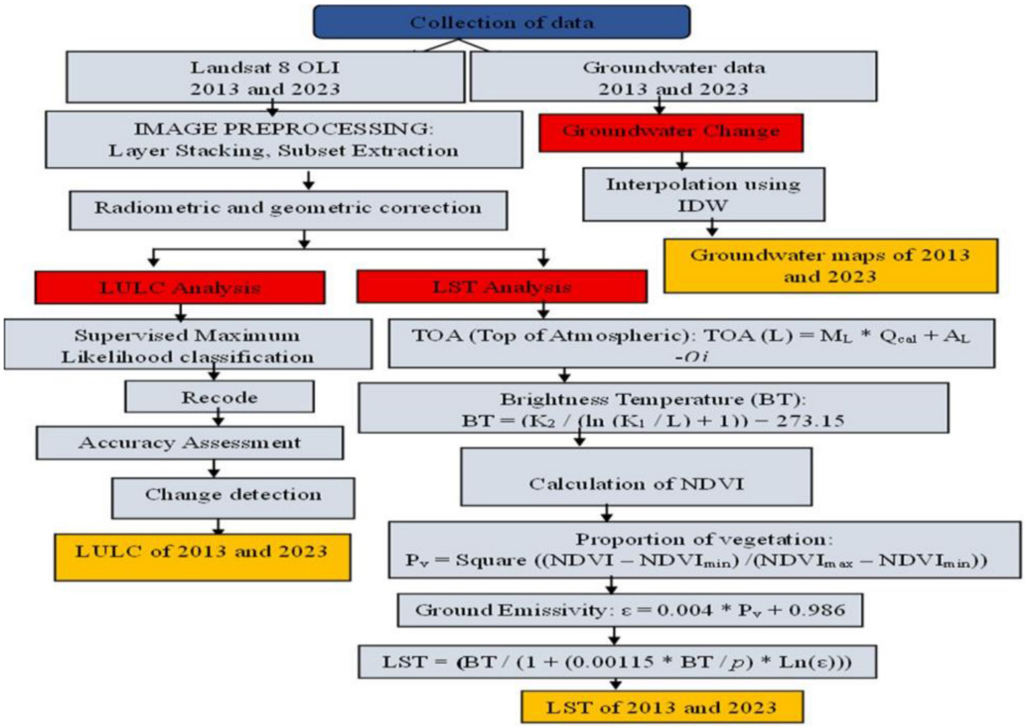

Fig. 2: Overview of Research Methodology

Table 2: LULC change detection

		2013 (Area in Km²)					
	LULC Classes	Agriculture	Barren	Built-up	Vegetation	Waterbody	Grand Total
2023 (Area in Km²)	Agriculture	581.69	23.67	13.25	29.50	6.18	654.28
	Barren	20.40	5.37	0.16	0.44	0.07	26.45
	Built-up	72.98	7.70	98.65	3.98	3.77	187.08
	Vegetation	16.97	0.45	3.24	15.74	1.55	37.96
	Waterbody	16.22	0.73	0.89	3.01	4.42	25.26
	Grand Total	708.27	37.92	116.18	52.67	15.99	931.02

surface parameter. The NDVI values are used to assess an element's average emissivity on the surface of the Earth. This can be expressed mathematically as follows: Eq. 6 (Sobrino *et al.,* 2004).

$$\varepsilon = 0.004 * P_v + 0.986 \quad \text{……………..(6)}$$

6- Calculation the Land Surface Temperature

The land surface temperature, also called the radiated temperature, is determined using the wavelength of the electromagnetic radiation emitted, the brightness temperature of the upper atmosphere, and the emissivity of the land surface (Guha *et al.,* 2018).

$$\mathrm{LST} = \mathrm{BT} / [1 + (\mathrm{W} * \mathrm{BT}/14380) * \ln(\varepsilon)] \quad \text{…………….(7)}$$

Where, BT = Top of atmosphere brightness temperature (°C), W = Emitted radiance Wavelength, E = Emissivity of the land Surface

Groundwater depth Interpolation Using Ordinary Kriging (OK)

Groundwater depth observations for May and November of 2013 and 2023 were spatially interpolated using the Ordinary Kriging (OK) method in ArcGIS 10.8 (Geostatistical Analyst extension). It is a geostatistical interpolation method that uses the spatial autocorrelation between adjacent observations to estimate the values at unsampled points. Ordinary Kriging does not use inverse distance weighting, but rather the spatial structure of the data is modelled with a semi-variogram, which generates statistically unbiased estimates with minimum estimation variance (Hasan *et al.,* 2021; Antonakos & Lambrakis, 2021). The predicted groundwater depth at an unsampled location is expressed as:

$$\hat{Z}(x_0) = \sum_{i=0}^{n} \lambda_i i Z(x_i) \quad \text{…………….(8)}$$

Where, , Z() is observed groundwater depth at the i[th] sampling location, n is number of neighboring observation points.

The kriging weights satisfy the unbiasedness constraint:

$$\sum_{i=0}^{n} \lambda_i = 1 \quad \text{…………………(9)}$$

The spatial dependence among groundwater observations is quantified using the experimental semi variogram:

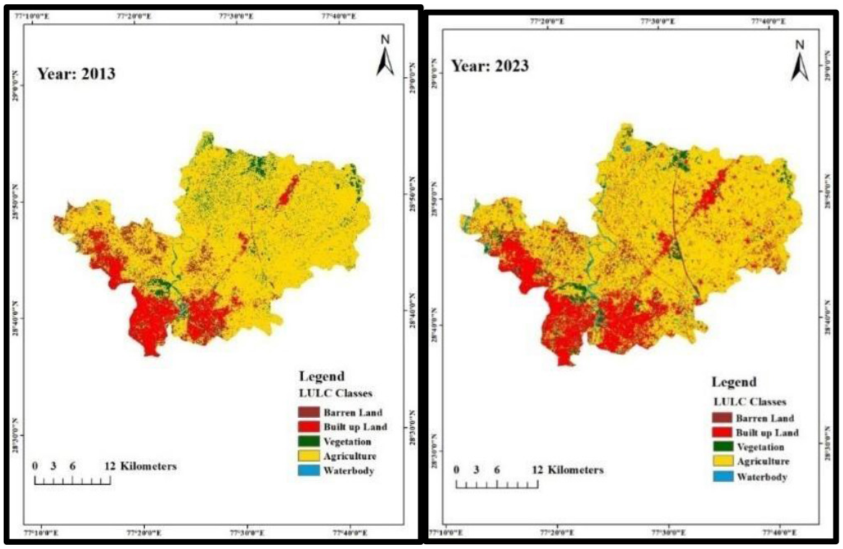

Fig. 3: LULC maps of Ghaziabad District for 2013 and 2023

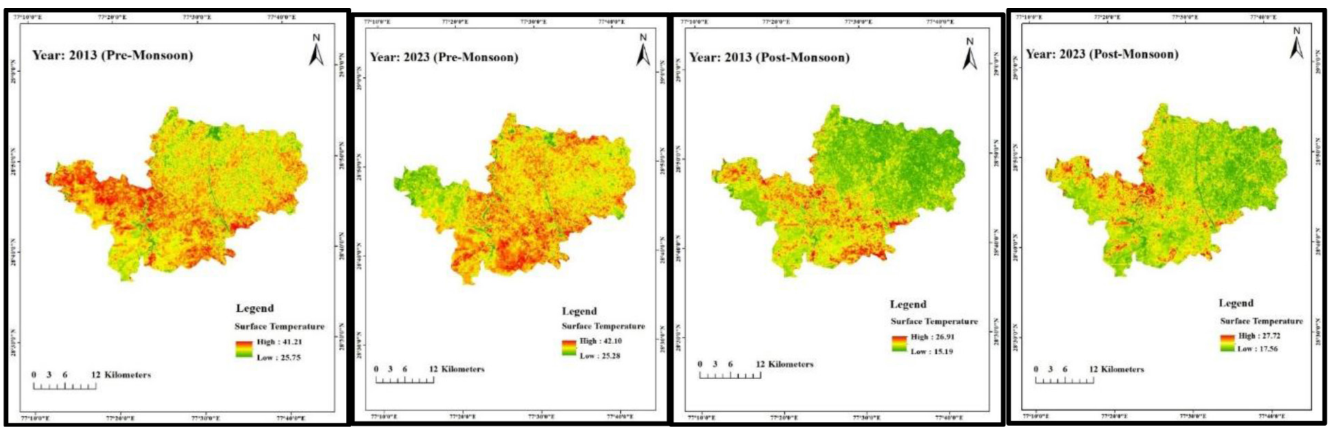

Fig. 4: Pre-Monsoon and Post-Monsoon LST maps of Ghaziabad District for 2013 and 2023

$$\gamma(h) = \frac{1}{2N(h)} \sum_{i=1}^{N(h)} [Z(X_i) - Z(X_i + h)]^2 \quad \ldots\ldots\ldots\ldots\ldots\ldots(10)$$

Where, $\gamma(h)$is semivariance at lag distance h, N(h) is number of data pairs separated by distance h, $[Z(X_i)$ and $Z(X_i+h)]$ is groundwater depth at locations separated by lag distance h.

The degree of accuracy of the Ordinary Kriging interpolations was validated through the leave-one-out cross-validation provided in ArcGIS Geostatistical Analyst. The Mean Error (ME), Root Mean Square Error (RMSE), Mean Standardized Error (MSE), Root Mean Square Standardized Error (RMSSE), and Average Standard Error (ASE) were used to measure the prediction performance.

RESULT

Land use and land cover (2013 and 2023)

The LULC maps for the years 2013 and 2023 are given in Fig. 3. It has been noted that during these years, the area of various LULC classes has altered. This shift in land use indicates a growth in urban areas and a decline in agriculture and vegetation. Rapid industrialization and urbanization caused LULC to undergo major transformation between 2013 and 2023. Consequently, between 2013 and 2023, the area percentage comprised of built-up land rose from 116.18 sq. km to 187.08 sq. km. In 2013, approximately 708.27 sq. km of the land was used for agriculture; by 2023, that percentage had sharply decreased to 654.28 sq. km. The amount of vegetated land declined from 2013 to 2023; it was 52.67 sq. km in 2013, and it declined to 37.96 sq. km in 2023. Roads, deforestation, and the rapid growth of human settlements are the main causes of the district's declining vegetation. Between 2013 and 2023, the area of barren land showed a decreasing trend, from 37.92 to 26.45 sq. km. Between 2013 and 2023, the built-up land area drastically increased from 116.18 sq. km to 187.08 sq. km. It is notable that there has been an overall rise in waterbody land from 2013 to 2023 (Table 2). Both of these expansions occurred at the expense of reduced bare and agricultural land, which accelerated the LST. The district's eastern and northeastern regions had substantial vegetation cover, whereas the western portion had a sizable amount of built-up area.

Accuracy assessment of the LULC classification

Table 3 summarizes the kappa coefficient of LULC categorization, user, producer, and overall accuracies. For 2013 and 2023, the overall classification accuracy of all classified images was 89% and 93%, respectively, suggesting a high degree of accuracy. The categorization of kappa in this research for all classified images

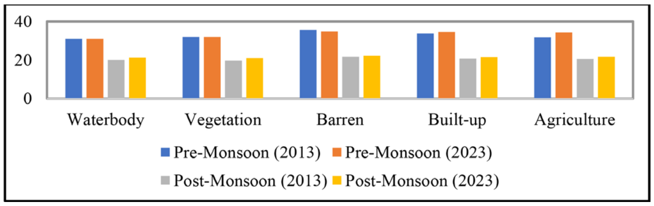

Fig. 5: Mean LST of Different LULC Classes

Table 3: Classification of accuracy assessment of LULC classes (2013 & 2023)

Classes	PA (2013)	UA (2013)	PA (2023)	UA (2023)
Built up	91%	97%	94%	97%
Barren	74%	93%	91%	97%
Vegetation	91%	97%	88%	91%
Waterbody	97%	100%	94%	94%
Agriculture	97%	73%	91%	91%
Overall Accuracy	89%	-	93%	-
Kappa Coefficient	86%	-	91%	-

PA=Producer Accuracy; UA=User Accuracy

was 86% and 91% for 2013 and 2023, falling within a range that is considered acceptable.

Spatio-temporal variations of land surface temperature (2013 and 2023)

Post-monsoon and pre-monsoon land surface temperature (LST) for Ghaziabad district has been calculated for various years, including 2013 and 2023. The highest temperature recorded during the pre-monsoon season ranged from 41^0 C in 2013 to 42^0 C in 2023, and there is no significant difference in the lowest temperature from 2013 to 2023. The highest recorded temperature during the post-monsoon season ranged from 26^0 C in 2013 to 27^0 C in 2023, while the lowest recorded temperature ranged from 15^0 C in 2013 to 17^0 C in 2023.

Because of urbanization, temperatures varied significantly throughout the Ghaziabad district. Between 2013 and 2023, the mean post-monsoon temperature rose substantially from 20.55^0 C to 21.66^0 C (Table 4). The maximum and minimum temperatures during the post-monsoon period from 2013 to 2023 were 2.37^0 C and 1^0 C, respectively, while the minimum temperature difference during the pre-monsoon period was not very significant, and the maximum temperature difference was roughly 1^0 C. The land surface temperature is substantially lower in the district's northeastern and eastern parts. In comparison to other portions of the study region, this area has somewhat more vegetation and agricultural land. The western portion of the district has a somewhat higher temperature than the rest of the district owing to the maximum concentration of built-up area in this direction (Fig. 4).

The mean LST for each LULC type rose in the post-monsoon during the study period. The pre-monsoon mean temperature did not significantly change between 2013 and 2023. Between 2013 and 2023, the pre-monsoon season mean LST of built-up land went up from 33.80 C to 34.550 C, whereas the mean LST of barren land rose from 31.850 C to 34.330 C. The mean land surface temperature of vegetation, waterbodies, and barren land did not vary significantly. The mean LST of built-up land rose from 20.790 C to 21.590 C in the post-monsoon period, whereas the mean LST of waterbodies, agricultural land, and barren land rose from 20.050 C to 21.590 C, 20.550 C to 21.730 C, and 21.730 C to 22.350 C, respectively, as illustrated in Fig. 5. According to LST figures, shifting land use has caused a steady increase in temperature since 2013. The urban area and its surroundings experience the biggest temperature differences, while areas with dense vegetation or water bodies have comparatively lower temperatures.

Analysis of groundwater fluctuations

Fig. 6 represents the spatial distribution of groundwater during the pre-monsoon (May) and post-monsoon (November) seasons of 2013 and 2023 using a common classification scale (5.90–21.71 mbgl) to reflect the direct comparison of seasonal and temporal groundwater variations. During the pre-monsoon of 2013 (Fig. 6A), deeper groundwater depths (18.00–21.71 mbgl) were concentrated in the central part of the district, whereas relatively shallow groundwater depths (5.90–9.00 mbgl) occurred mainly in the northern and northeastern regions. Progressive groundwater depletion across the district is shown on the pre-monsoon map (Fig. 6B) by a progressive increase in groundwater depth classes 15.00-18.00 mbgl and 18.00-21.71 mbgl, especially in the central and southwestern portion of the district. In the post-monsoon (Fig. 6C), shallow groundwater classes became more common, reflecting recharge during the monsoon season, although deeper groundwater classes remained in the central city. The post-monsoon map (Fig. 6D) showed that the groundwater recovered partially in the monsoons, but the deeper groundwater classes still dominated in the urban core, indicating that groundwater abstraction was not balanced by groundwater recharge due to the monsoons. Overall, the comparison shows that groundwater depth has increased from 2013 to 2023, resulting from the combined impacts of rapid urbanization, increased groundwater pumping, and decreased infiltration resulting from the increase in impervious surfaces. The results emphasize the requirement for sustainable use of groundwater, such as artificial recharge and rainwater harvesting, to reduce long-term groundwater depletion.

Groundwater depth Ordinary Kriging cross-validation statistics and semivariogram parameters for pre-monsoon (May) and post-monsoon (November) 2013 and 2023 seasons are shown in Table 5. Across all datasets, ME ranged from −2.499 to −2.999 m, RMSE from 6.080 to 6.519 m, MSE from −0.207 to −0.227, RMSSE from 0.698 to 0.756, and ASE from 5.579 to 6.442 m. An exponential semivariogram model with a nugget value of zero, a partial sill value of 102.156 to 136.225, and a range value of 107,356.189 m was used. The cross-validation results show that the systematic prediction bias is low and the interpolation results are moderately consistent; however, because there are only four piezometric observation wells in this cross-validation, the maps should be viewed as generalized spatial patterns and not as a precise continuous groundwater surface.

DISCUSSION

The LULC based on 2013-2023 data showed that built-up areas have increased considerably in Ghaziabad District, while

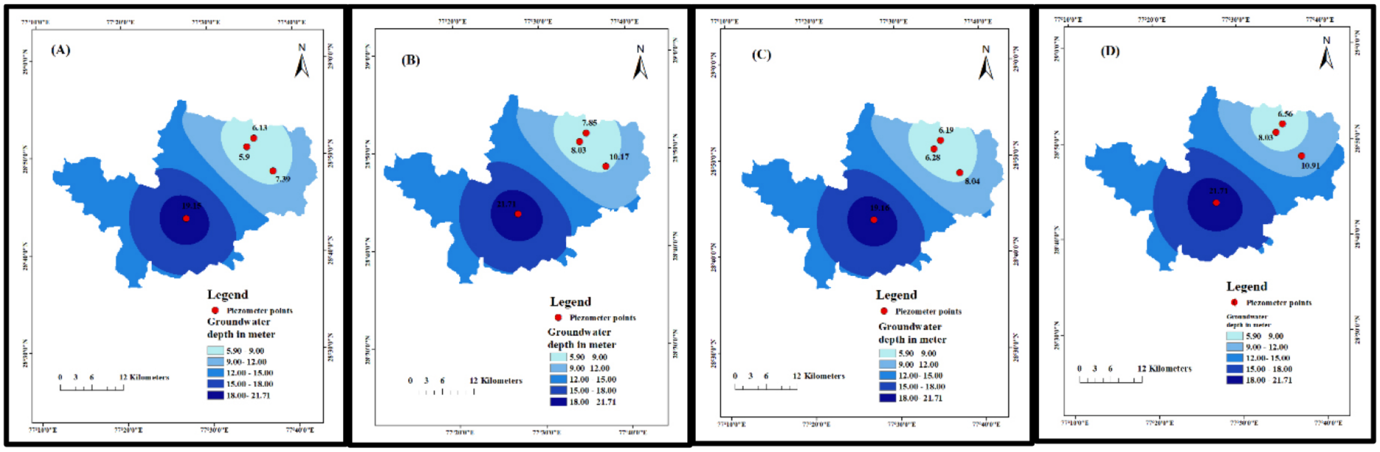

Fig. 6: Seasonal spatial distribution of groundwater depth (m below ground level, mbgl) in Ghaziabad District: (A) Pre-monsoon 2013 (May), (B) Pre-monsoon 2023 (May), (C) Post-monsoon 2013 (November), (D) Post-monsoon 2023 (November)

Table 5: Cross-validation statistics and semivariogram parameters of Ordinary Kriging interpolation for groundwater depth (2013 and 2023)

Season	Pre-monsoon 2013 (May)	Post-monsoon 2013 (November)	Pre-monsoon 2023 (May)	Post-monsoon 2023 (November)
Samples	4	4	4	4
ME (m)	-2.536	-2.499	-2.676	-2.999
RMSE (m)	6.346	6.08	6.392	6.519
MSE	-0.207	-0.21	-0.213	-0.227
RMSSE	0.756	0.733	0.724	0.698
ASE (m)	5.698	5.579	5.934	6.442
Semivariogram Model	Exponential	Exponential	Exponential	Exponential
Nugget	0	0	0	0
Partial Sill	106.567	136.225	102.156	115.601
Range (m)	107356	107356	107356	107356

ME = Mean Error; RMSE = Root Mean Square Error; MSE = Mean Standardized Error; RMSSE = Root Mean Square Standardized Error; ASE = Average Standard Error.

vegetation and agricultural areas have decreased. The changes have been observed consistently with the urbanization observed in other rapidly growing cities of India that are experiencing rapid industrialization, population growth, and infrastructure development (Naikoo *et al.,* 2020). The expansion of built-up land was accompanied by an evident rise in land surface temperature (LST), especially in highly populated urban zones. The increased impervious surfaces like concrete and asphalt over natural land cover increase heat absorption and storage, which worsens the urban heat island (Pushkar *et al.,* 2025). However, vegetated and agricultural areas had relatively low LST values, attributable to evaporation and shading, which emphasizes the significance of the cooling effect of urban green spaces (Guha & Govil, 2025). The reduction in agricultural land and expansion of built-up areas represent growing stress on the agricultural environment in Ghaziabad District. These changes, when added to the increase in temperature of the land surface and the rise in groundwater depth, could affect irrigation needs and the long-term viability of agricultural production. Thus, urban development that is integrated with sustainable land and water resource management is needed to reduce negative effects on agriculture. Groundwater analysis indicated a progressive decline in groundwater conditions, particularly in urbanized areas. The interpolation was made from four observation wells, but the spatial pattern indicates that deeper groundwater occurs in built-up areas than in less built-up areas. As impervious surfaces increase, infiltration and groundwater recharge decrease and domestic, industrial, and commercial water consumption increase, which leads to increased groundwater abstraction. Verma *et al.,* (2020) have also reported similar relations between urbanization, decrease in recharge, and groundwater depletion. Resulting from the integrated assessment, there is a strong linkage between the change in LULC, LST, and groundwater fluctuations. Higher groundwater depth and LST were generally observed in areas with predominantly built-up land use, while areas with more vegetation have comparatively low temperatures and better groundwater conditions. This finding aligns with Jadhav *et al.,* (2023), who found that urbanization has a significant impact on groundwater resources and climatic conditions. The overall findings highlight the critical importance of sustainable urban planning approaches, such as implementing green infrastructure, afforestation, rainwater harvesting, and artificial groundwater recharge, to help reduce thermal stress, increase groundwater sustainability, and boost urban resilience in rapidly urbanizing districts. The cross-validation results indicate that the Ordinary Kriging interpolation provided a reasonably consistent representation of seasonal groundwater depth variations during both the pre-monsoon (May) and post-monsoon (November) periods in 2013 and 2023. Although prediction bias remained low, the limited number of piezometric observation wells (n = 4) constrained the robustness of the semivariogram and increased interpolation uncertainty. Consequently, the interpolated groundwater depth maps are best interpreted as illustrating broad seasonal and temporal spatial trends rather than highly accurate groundwater surfaces. Expanding the groundwater monitoring network would improve interpolation reliability and reduce prediction uncertainty in future studies.

CONCLUSION

The objective of this study was to evaluate the spatio-temporal variation of LULC, LST, and groundwater depth in the Ghaziabad District using Remote Sensing and GIS for the period 2013-2023. The results indicated that the built-up area in 2023 was 187.08 km2 (12.25% of the total district area), which was higher than 116.18 km2 (7.60% of the total district area) in 2013, while the vegetation and agricultural land decreased. Higher LST was found to be associated with urbanization, especially in highly urbanized areas, and groundwater depth increased gradually in both pre- and post-monsoon seasons. The results show that thermal stress and groundwater depletion have been exacerbated by high urbanization rates. The results also indicate that the current trend of urban growth may lead to decreased availability of agricultural land and greater pressure on irrigation water supplies, highlighting the need for sustainable land-use and groundwater management to ensure agricultural sustainability. Hence, sustainable urban planning, recharge of groundwater, harvesting of rainwater, and green infrastructure are crucial to address future environmental issues in Ghaziabad District.

LIMITATIONS OF THE STUDY

The study was restricted to four groundwater observation wells, and secondary groundwater data may not completely capture the spatial variability of groundwater conditions in Ghaziabad District. Therefore, the Ordinary Kriging maps should be viewed as general groundwater depth trends, not as exact district-wide values, and further studies should use a more robust groundwater monitoring network and field observations over time to increase the reliability of interpolation and the strength of the groundwater assessment.

ACKNOWLEDGEMENT

In preparing this manuscript, the author did not receive any particular support or help that has to be acknowledged.

Author's certificate: The manuscript or its part is not under consideration for publication elsewhere and the same has been approved by all co-authors.

Conflict of Interests: The authors declare that there is no conflict of interest regarding the publication of this article.

Funding: This research did not receive any specific funding.

Data Availability: The data supporting the findings of this study are accessible from the authors upon reasonable request.

Authors contribution: **Sadaf:** The author confirms being the sole contributor of this work, including Data curation, Formal analysis, Methodology; editing, Writing-original draft, Methodology, Investigation, review and formal analysis.

Disclaimer: The contents, opinions, and views expressed in the research article published in the Journal of Agrometeorology are the views of the authors and do not necessarily reflect the views of the organisations they belong to.

Publisher's Note: The periodical remains neutral concerning jurisdictional claims in published maps and institutional affiliations.

REFERENCES

Aman, A., Randriamanantena, H. P., Podaire, A., & Froutin, R. (1992). Upscale Integration of Normalized Difference Vegetation Index: The Problem of Spatial Heterogeneity. *IEEE Transactions on Geoscience and Remote Sensing*, *30*, 326-338. https://doi.org/10.1109/36.134082.

Anand, S., Bhati A., Singh, P., Singh, A., Mayala, V. K., & Kumar, H. (2024). Spatio-Temporal Change of Landscape and Its Impact on Agriculture Development in Ghaziabad District. *Current Agriculture Research Journal*, *12*(3). http://dx.doi.org/10.12944/CARJ.12.3.25

Antonakos, A., & Lambrakis, N. (2021). Spatial Interpolation for the Distribution of Groundwater Level in an Area of Complex Geology Using Widely Available GIS Tools. *Environmental Processes, 8,* 993–1026. https://doi.org/10.1007/s40710-021-00529-9.

Battista, G. & De Lieto Vollaro, R. (2017). Correlation between air pollution and weather data in urban areas: Assessment of the city of Rome (Italy) as spatially and temporally independent regarding pollutants. *Atmospheric Environment*, *165,* 240-247. https://doi.org/10.1016/j.atmosenv.2017.06.050.

Carlson, T. N., & Ripley, D. A. (1997). On the relation between NDVI, fractional vegetation cover, and leaf area index. *Remote Sensing of Environment*, *62*(3), 241–252.

Central Ground Water Board. (2023). *Ground Water Year Book Uttar Pradesh*. Ground Water Department, Government of Uttar Pradesh.

Cohen, J. (1960). A coefficient of agreement for nominal scales. *Educational and Psychological Measurement, 20*. https://doi.org/10.1177/001316446002000104.

Guha, S., Govil, H., Dey, A., & Gill, N. (2018). Analytical study of land surface temperature with NDVI and NDBI using Landsat 8 OLI and TIRS data in Florence and Naples city, Italy. *European Journal of Remote Sensing, 51*(1), 667–678. https://doi.org/10.1080/22797254.2018.1474494

Guha, S., & Govil, H. (2025). Evaluating the stability of the relationship between land surface temperature and land use/land cover indices: a case study in Hyderabad city, India. *Geology, Ecology, and Landscapes, 9*(1), 231–243. https://doi.org/10.1080/24749508.2023.2182083.

Hasan, K., Paul, S., Chy, T. J., & Antipova, A. (2021). Analysis of groundwater table variability and trend using ordinary kriging: the case study of Sylhet, Bangladesh. *Applied Water Science, 11,* 120. https://doi.org/10.1007/s13201-021-01454-w.

Jadhav, P., Manekar, V. L., & Patel, J. N. (2023). Spatiotemporal Land Use Land Cover Change Impacts on Groundwater Table in Surat District, India. In T P. V. Timbadiya, P. L. Patel, V. P. Singh, & A. B. Mirajkar (Eds.), *Geospatial and Soft Computing Techniques* (pp 101–112). Springer. https://doi.org/10.1007/978-981-99-1901-7_10.

Moharir, K. N., Baliram Pande, C., Gautam, V. K., Dash, S. S., Mishra, A. P., Yadav, K. K., Darwish, H. W., Pramanik, M., & Elsahabi, M. (2025). Estimation of land surface temperature and LULC changes impact on groundwater resources in the semi-arid region of Madhya Pradesh, India. *Advances in Space Research, 75*(1), 233–247. https://doi.org/10.1016/j.asr.2024.09.025.

Naikoo, M.W., Rihan, M., Ishtiaque, M., & Shahfahad. (2020). Analyses of land use land cover (LULC) change and built-up expansion in the suburb of a metropolitan city: Spatio-temporal analysis of Delhi NCR using landsat datasets. *Journal of Urban Management*, *9*(3), 347-359. https://doi.org/10.1016/j.jum.2020.05.004.

Patra, S., Sahoo, S., Mishra, P., & Mahapatra, S.C. (2018). Impacts of urbanization on land use/cover changes and its probable implications on local climate and groundwater level. *Journal of Urban Management, 7,* 70-84. https://doi.org/10.1016/j.jum.2018.04.006

Pushkar, D. S., Mishra, A., Arya, D. S., Jaiswal, S., & Kumar, A. (2025). Investigating the effects of land use, land cover change, and urban heat island effects in Agra city, India, using a remote sensing approach. *Discover Cities, 2,* 105. https://doi.org/10.1007/s44327-025-00149-0.

Ramaiah, M., Avtar, R., & Rahman, M. M. (2020). Land Cover Influences on LST in Two Proposed Smart Cities of India: Comparative Analysis Using Spectral Indices. *Land*, *9*(9):292. https://doi.org/10.3390/land9090292.

Rouse, J. W., Hass, R. H., Schell, J. A., Deering, D. W., & Harlan, J. C. (1974). Monitoring the Vernal Advancement and Retrogradation (Greenwave Effect) of Natural Vegetation. *NASA/GSFC Type III Final Report*. Greenbelt, MD: NASA/ GSFC.

Sobrino, J. A., Jiménez-Muñoz, J. C., & Paolini, L. (2004). Land surface temperature retrieval from Landsat TM 5. *Remote Sensing of Environment*, *90*(4), 434–440.

Saha, J., Ria, S. S., Sultana, J., Shima, U. A., Seyam, M. M. H., & Rahman, M. M. (2024). Assessing seasonal dynamics of land surface temperature (LST) and land use land cover (LULC) in Bhairab, Kishoreganj, Bangladesh: A geospatial analysis from 2008 to 2023. *Case Studies in Chemical and Environmental Engineering, 9,* 100560. https://doi.org/10.1016/j.cscee.2023.100560.

Singh, A., & Mishra, V. N. (2020). Estimation of changes in land surface temperature using multi-temporal Landsat data of Ghaziabad District, India. *Forum geographic, 19*(1), 45-59. http://dx.doi.org/10.5775/fg.2020.040.i

Tyagi, S., & Sharma K. (2021). Seasonal variability, index modeling and spatiotemporal profiling of groundwater usability in semi-urban region of Western Uttar Pradesh, India. *Environmental Earth Sciences, 80,* 761. https://doi.org/10.1007/s12665-021-10018-9.

Uttar Pradesh Ground Water Department (2022). *Pre-monsoon and Post-monsoon Ground Water Level Data (In Mbgl).* Ground Water Department, Government of Uttar Pradesh. http://upgwd.gov.in/MediaGallery/WLD08092017.pdf. Accessed 16 Nov 2020

Verma, P., Singh, P., & Srivastava, S. K. (2020). Impact of land use change dynamics on sustainability of groundwater resources using earth observation data. *Environment, Development and Sustainability, 22*(6), 5185–5198.

Wang, W., Zhang, Z., Duan, L., Wang, Z., Zhao, Y., Zhang, Q., Dai, M., Liu, H., Zheng, X., & Sun, Y. (2018). Response of the groundwater system in the Guanzhong Basin (central China) to climate change and human activities. *Hydrogeology Journal*, *26*(5), 1429-1441. https://doi.org/10.1007/s10040-018-1757-7

Zahran, H., Ali, M. Z., Jadoon, K. Z., Yousafzai, H. U. K., Rahman, K. U., & Sheikh, N. A. (2023). Impact of Urbanization on Groundwater and Surface Temperature Changes: A Case Study of Lahore City. *Sustainability*, *15*(8), 6864. https://doi.org/10.3390/su15086864.